

This is the accepted manuscript made available via CHORUS. The article has been published as:

# First Detection of Scale-Dependent Linear Halo Bias in N-Body Simulations with Massive Neutrinos

Chi-Ting Chiang, Marilena LoVerde, and Francisco Villaescusa-Navarro

Phys. Rev. Lett. **122**, 041302 — Published 1 February 2019

DOI: [10.1103/PhysRevLett.122.041302](https://doi.org/10.1103/PhysRevLett.122.041302)

# First detection of scale-dependent linear halo bias in $N$ -body simulations with massive neutrinos

Chi-Ting Chiang,<sup>1,2</sup> Marilena LoVerde,<sup>1</sup> and Francisco Villaescusa-Navarro<sup>3</sup>

<sup>1</sup>*C.N. Yang Institute for Theoretical Physics, Department of Physics & Astronomy,  
Stony Brook University, Stony Brook, NY 11794*

<sup>2</sup>*Physics Department, Brookhaven National Laboratory, Upton, NY 11973, USA*

<sup>3</sup>*Center for Computational Astrophysics, Flatiron Institute, 162 5th Avenue, 10010, New York, NY, USA*

Using  $N$ -body simulations with massive neutrino density perturbations, we detect the scale-dependent linear halo bias with high significance. This is the first time that this effect is detected in simulations containing neutrino density perturbations on all scales, confirming the same finding from separate universe simulations. The scale dependence is the result of the additional scale in the system, i.e. the massive neutrino free-streaming length, and it persists even if the bias is defined with respect to the cold dark matter plus baryon (instead of total matter) power spectrum. The separate universe approach provides a good model for the scale-dependent linear bias, and the effect is approximately  $0.25f_\nu$  and  $0.43f_\nu$  for halos with bias of 1.7 and 3.5, respectively. While the size of the effect is small, it is *not* insignificant in terms of  $f_\nu$  and should therefore be included to accurately constrain neutrino mass from clustering statistics of biased tracers. More importantly, this feature is a distinct signature of free-streaming particles and cannot be mimicked by other components of the standard cosmological model.

Massive neutrinos play an important role in cosmology. They contribute to the energy budget, which impacts the expansion history, and their large momenta prevent them from clustering along with cold dark matter (CDM) on scales smaller than their free-streaming length,  $\lambda_{\text{fs}}$ . As a result, the growth of matter fluctuations becomes *scale-dependent*, with fluctuations on sub-free-streaming scales growing more slowly. This effect suppresses the matter power spectrum for  $k > k_{\text{fs}} \sim 1/\lambda_{\text{fs}}$  by an amount proportional to the fraction of the matter budget composed of neutrinos  $f_\nu$  [1, 2]. Since the neutrino abundance is fixed by the cosmology and deviations are well-constrained [3], a detection of this effect determines the sum of the neutrino masses,  $\sum m_\nu$ .

Scale-dependent growth of structure from neutrinos also fundamentally changes the way that the halo (or galaxy or cluster) density field traces the underlying matter distribution. The relationship between the two can be parameterized by a bias coefficient  $b$ , with  $\delta_h \sim b\delta_c$ , where  $\delta_h$  is the halo number density contrast and  $\delta_c$  the CDM+baryon density contrast. In the standard  $\Lambda$ CDM cosmology, halo formation is completely local and this dictates that the bias approaches a constant on large-scales [4–7]. Neutrinos, however, can travel cosmological distances during structure formation. Consequently, the local gravitational dynamics of particles forming halos depends upon the history of neutrino density field out to extremely large scales. This fact allows the halo bias to become scale-dependent, where the scale introduced is the neutrino free-streaming scale. Since the bias is itself an observable, this effect offers another probe of  $\sum m_\nu$ .

Scale-dependent bias generated by massive neutrinos was first predicted by Ref. [8], and later measured in  $N$ -body simulations using the separate universe technique in Ref. [9]. A related effect on the bias of cosmic voids

was identified in Ref. [10]. The effect on halos has not yet been detected by any other neutrino simulation techniques for two main reasons. First, to robustly detect quantities of  $\mathcal{O}(f_\nu)$ , a statistical error bar of  $\mathcal{O}(f_\nu/5)$  is needed. This is challenging because current constraints on  $\sum m_\nu$  correspond to  $f_\nu \lesssim 0.01$ . Typically  $f_\nu$  is artificially boosted to increase the amplitude of neutrino effects by increasing the neutrino mass [11–29], rather than the number density. This has the effect of pushing the free-streaming scale towards the nonlinear scale where there are other, more mundane, sources of scale dependence that are hard to disentangle. Second, since the bias effect arises from the sensitivity to neutrino perturbations at earlier epochs when the comoving free-streaming length was larger, very large volume simulations are needed. Specifically, for a relatively light neutrino mass (e.g. 0.05eV, which gives  $\lambda_{\text{fs}} \sim 200\text{Mpc}$  today) Gpc-scale simulations are needed. These simulations exist, but none of them have had the statistical power to detect this effect [20–29].

In this letter, we perform simulations with neutrino density perturbations that meet the above requirements. The degenerate neutrino mass is set to  $m_\nu = 0.05\text{eV}$ , so that  $\lambda_{\text{fs}}$  is large enough and the nonlinear contamination is limited. This choice also gives a free-streaming scale consistent with that from the minimal mass of the normal and inverted mass orderings, and expectations given current cosmological constraints ( $\sum m_\nu \leq 0.12\text{eV}$  at 95% [3]). To enhance  $f_\nu$  so that effects can be probed by a reasonable number of simulations, we increase the number of neutrino species to  $N_\nu = 28$  to give  $f_\nu \approx 0.1$ .<sup>1</sup> We set the size of the simulation box to  $L = 4000h^{-1}\text{Mpc}$

<sup>1</sup> We choose  $f_\nu \approx 0.1$  so that the effect is large enough to be

to probe the bias out to the largest scales. Cosmological parameters are as follows: Hubble constant  $h = 0.7$ , baryon density  $\Omega_b = 0.05$ , CDM density  $\Omega_c = 0.25$ , CMB temperature  $T_\gamma = 2.725\text{K}$ , helium fraction  $Y_{\text{He}} = 0.24$ , the initial curvature power spectrum with the spectral index  $n_s = 0.95$ , and the amplitude which sets  $\sigma_8 = 0.83$  today for the power spectrum of CDM+baryon field.

These simulation choices pose two challenges. First, for such light neutrino masses, a substantial fraction of neutrinos are relativistic at the simulation starting redshift (e.g. at  $z_i = 99$ ,  $\rho_\nu(a_i)/(\rho_{\nu,0}a_i^{-3}) \sim 1.5$ ). Thus, simulation methods that treat neutrinos as non-relativistic particles can lead to unphysical effects.<sup>2</sup> Second, on the largest scales, radiation perturbations become important, and ignoring them will lead to incorrect growth (see, e.g. Ref. [31]). To address these problems, we include neutrino and photon perturbations on grids in our gravity solver [32]. Concretely, the dynamics of the CDM+baryon field is carried out by **Gadget-2** [33], and we modify the particle-mesh (PM) potential as

$$\Phi_{\text{tot}}(k, a) = \Phi_{bc}(k, a) \left\{ 1 + 2 \frac{f_\gamma(a)}{f_{bc}(a)} \frac{T_\gamma(k, a)}{T_{bc}(k, a)} + \frac{f_\nu(a)}{f_{bc}(a)} \frac{T_\nu(k, a)}{T_{bc}(k, a)} [1 + 3c_{s,\nu}^2(a)] \right\}. \quad (1)$$

Here,  $\Phi_{bc}$  is the CDM+baryon potential computed from the simulation particles,  $f_x = \bar{\rho}_x/(\bar{\rho}_\gamma + \bar{\rho}_\nu + \bar{\rho}_{bc})$ ,  $T_x$  is the linear transfer function computed by **CLASS** [34, 35], and we approximate the neutrino sound speed  $c_{s,\nu}^2(a) \approx \dot{\rho}_\nu(a)/\dot{P}_\nu(a)$  [35, 36]. Since baryons are treated as CDM in simulations, hereafter CDM can refer to CDM+baryons. CDM particles are then displaced according to  $\Phi_{\text{tot}}$ , instead of  $\Phi_{bc}$ , to account for the photon and neutrino perturbations. We repeat the procedure at each time step for the long-range force calculation. The simulation initial conditions are set up using the Zel'dovich approximation [37] with the CDM+baryon linear power spectrum and the scale-dependent growth rate computed by **CLASS** at  $z_i = 99$ . We set the number of particles sampling CDM+baryon perturbations and PM grids to be  $1536^3$  and  $4096^3$ , respectively.

The accuracy of this approach relies on two assumptions. First, photon and neutrino perturbations are neglected on scales smaller than the PM grid size:  $\sim 1h^{-1}$  Mpc. This is a good approximation because the size of the PM grid is much smaller than the neutrino

free-streaming scale and the photon free-streaming scale (the Hubble radius) at all redshifts of interest. Second, while linear photon and neutrino perturbations of mode  $k$  can affect the nonlinear evolution of CDM particles of the same  $k$ , nonlinear evolution of neutrino and photon perturbations is ignored. Relatedly, our calculation of the total potential assumes that the photon and neutrino perturbations have the same phases as CDM+baryon perturbations on all scales. By construction, for our neutrino mass  $\lambda_{\text{fs}} \sim 200\text{Mpc}$  today, which is large in comparison to the nonlinear scale ( $\sim 10\text{Mpc}$ ) and also the Lagrangian radii of halos ( $\lesssim 10\text{Mpc}$ ). At higher redshift, and for photons, the free-streaming scales are even larger, so corrections from the nonlinear photon and neutrino perturbations should be negligible. Moreover, it has been shown in Refs. [20, 38–41] that neutrino clustering around halos is negligible as long as the individual neutrino masses have  $m_\nu \lesssim 0.2\text{eV}$ . To check the performance of our modification, we compare the CDM+baryon power spectrum computed from simulations and **CLASS** at  $z = 1$  and  $0$ . On linear scales of  $1.57 \times 10^{-3} \leq k/(h \text{ Mpc}^{-1}) \leq 10^{-2}$ , the fractional difference is less than 0.5%,<sup>3</sup> which is smaller than the effect that we are targeting.

We identify halos using the Amiga Halo Finder [42, 43]. Since there are no neutrino particles in the simulations, halos are identified using CDM particles alone. We set the density threshold to  $\Delta = 200$ , and the minimum number of particles in halos to be 20. We split the dark matter halos between two catalogs:  $2.75 \times 10^{13} \leq M_h/(h^{-1} M_\odot) < 2.75 \times 10^{14}$  and  $2.75 \times 10^{14} \leq M_h/(h^{-1} M_\odot) < 2.75 \times 10^{15}$ . The halo bias is defined as

$$b(k) = P_{hc}(k)/P_{cc}(k), \quad (2)$$

where  $P_{hc}$  and  $P_{cc}$  are respectively the halo-CDM and CDM-CDM power spectra measured from simulations. This definition greatly reduces the scale dependence of the bias in comparison with a bias defined with respect to the total (neutrino and CDM+baryon) matter density field [8, 21, 22, 44]. The alternative bias definition is appropriate when combining galaxy and lensing data and can provide additional constraints on neutrino mass [45–47]. In addition to the massive neutrino simulations, we also run simulations with a reference cosmology *without* (massive or massless) neutrinos. The rest of the procedures and cosmological parameters are identical to simulations with massive neutrinos. In particular, photon perturbations are included in the potential in eq. (1) and the scale-dependent CDM+baryon linear

detected by a reasonable amount of simulations, and is small enough so that the neutrino effects are linear in  $f_\nu$ .

<sup>2</sup> One would have to wait until  $z \sim 10$  for half of the neutrino population to be non-relativistic ( $p \lesssim 0.1m_\nu$ , say); simulations with late starting redshifts will be inaccurate due to transients from initial conditions [30], which may well be systematically different between simulations with and without massive neutrinos.

<sup>3</sup> One cannot achieve this level of agreement between simulations and Boltzmann code if photon and neutrino perturbations are not included. See e.g. Ref. [31] for the large-scale difference between the full Boltzmann calculation and the two-fluid approximation without including radiation perturbations.

power spectrum and growth rate are used to set the initial conditions.

Note that while we fix the value of  $\sigma_8$  of the CDM+baryon power spectrum to be the same today for the two cosmologies, this does not make the two power spectra the same since they have different shapes. For a fixed  $\sigma_8$ , the massive neutrino cosmology has a larger power spectrum for  $k \ll k_{\text{fs}}$  and a slightly smaller power spectrum on smaller scales. This difference makes the function  $\sigma(M_h)$ , the variance of perturbations smoothed on scale  $R \sim (M_h/\rho_c)^{1/3}$ , different at all redshifts, with the massive neutrino cosmology having a larger amplitude  $\sigma(M_h)$  at the high-mass end and smaller  $\sigma(M_h)$  at the low mass end.<sup>4</sup> As a result, halos of the same mass will have different abundances and different bias factors in each cosmology.

Figure 1 shows the halo bias measured from 40 simulations with neutrinos (black circles) and without neutrinos (magenta triangles). The error bars show the error on the mean. From top to bottom the panels show the results for the halo catalogs of a low-mass bin at  $z = 0$ , a high-mass bin at  $z = 0$ , and a low-mass bin at  $z = 1$ . The error bars are much larger for high-mass halos at  $z = 1$  due to their rarity, so we do not show the result. The most obvious feature in figure 1, is the difference in the overall amplitude of the bias between the two cosmologies. As discussed, this is to be expected from the difference in  $\sigma(M_h)$  and we find good agreement with numerical predictions for halo bias that take  $\sigma(M_h)$  as input (e.g. Ref. [48]). **In particular, the relative amplitude of  $\sigma(M_h)$  for the two cosmologies flips between low- and high-mass halos, resulting a change in bias amplitude seen in figure 1.** The differences in the errors on the bias are also in agreement with the analytic calculations that take the stochasticity between the halo and matter fields to be inversely proportional to the number density of halos, giving  $\sigma_b^2 \propto 1/(nP_{cc})$ . **For the halos in figure 1, the difference in the power spectra dominates the difference in the error bars and our parameter choices give a larger  $P_{cc}$  in the massive neutrino cosmology, resulting in smaller errors on the bias on these scales for both mass bins.**

At present, the amplitude of the bias is not predicted with sufficient accuracy to extract reliable constraints on neutrino mass so it is usually treated as a free parameter in cosmological analyses. Given this, we move on to examine the scale dependence of the bias. At the highest  $k$ , the bias in both cosmologies has an upturn consistent with  $k^2$  and  $k^4$  bias terms [49, 50], the amplitudes of which are also typically treated as free parameters that do not constrain cosmology [51]. The most interesting

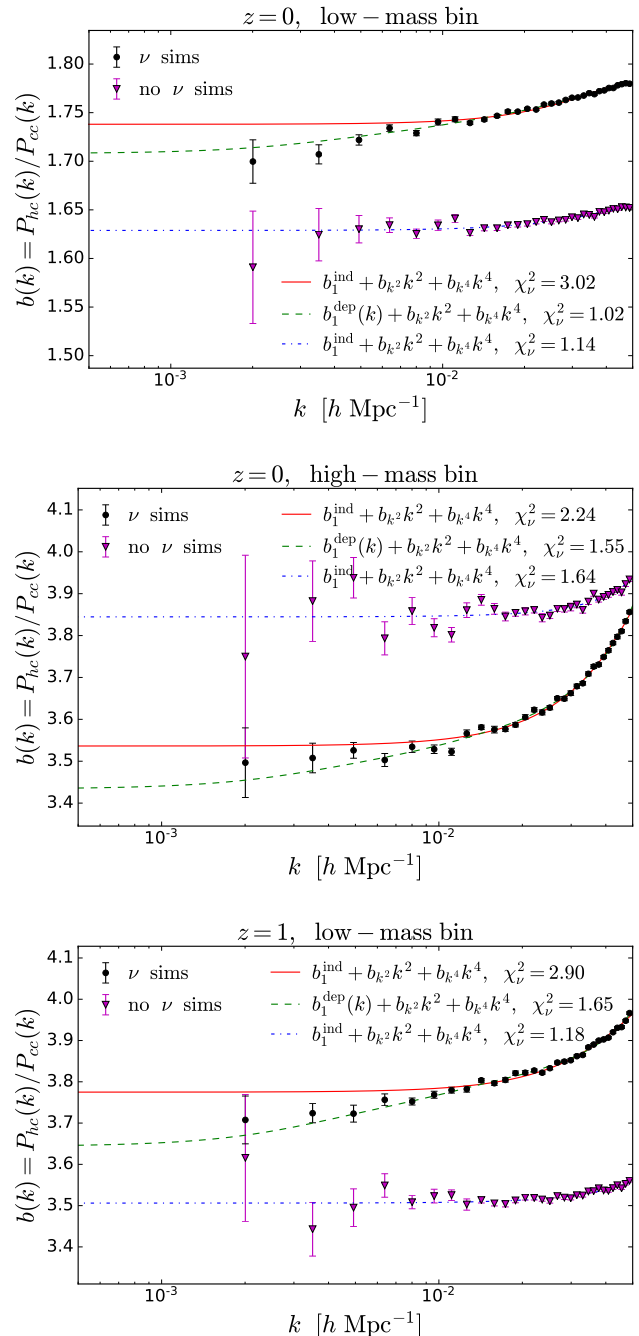


FIG. 1. Halo bias measured from 40 simulations with (black circles) and without massive neutrinos (magenta triangles). The errors bars show the error on the mean. From top to bottom: low-mass bin at  $z = 0$ , high-mass bin at  $z = 0$ , low-mass bin at  $z = 1$ . Each panel shows the best fits for the bias in the massive neutrino simulations using the scale-independent (red solid) and scale-dependent (green dashed) models in eq. (3) and eq. (4). The blue dot-dashed lines show the best-fit bias for the no-neutrino simulations using the scale-independent model in eq. (3). The fits are performed within  $1.57 \times 10^{-3} \leq k/(h \text{ Mpc}^{-1}) \leq 5 \times 10^{-2}$ . The reduced  $\chi^2_\nu$  values shown in the legend are estimated from *variance only*.

<sup>4</sup> The absence of neutrinos contributing to the global energy density also changes the expansion history, which changes the redshift evolution of  $\sigma_8(z)$ ,  $\sigma(M_h, z)$ , but this effect is subdominant.

feature in figure 1, however, is the persistent difference in the  $k$ -dependence of the biases at larger scales (e.g.  $k \sim 10^{-3} - 10^{-2} h \text{ Mpc}^{-1}$ ). These scales are well into the linear regime and are therefore robust to nonlinear contamination and baryonic effects. We fit the measurements to two different bias models: (i) a model with scale-independent linear bias,

$$b(k) = \underbrace{b_1}_{\equiv b_1^{\text{ind}}} + b_{k^2} k^2 + b_{k^4} k^4, \quad (3)$$

and (ii) a scale-dependent model

$$b(k) = 1 + \underbrace{(b_1 - 1)f(k)}_{\equiv b_1^{\text{dep}}(k)} + b_{k^2} k^2 + b_{k^4} k^4. \quad (4)$$

In both models there are three free parameters,  $b_1$ ,  $b_{k^2}$ , and  $b_{k^4}$ , each are fit separately for every mass bin, redshift, and cosmology. The factor  $f(k)$  in eq. (4) is a redshift- and cosmology-dependent function, taken from the separate universe prediction for how the local power spectrum changes in response to a long-wavelength CDM+baryon perturbation  $\delta_c(k)$  [9].<sup>5</sup> Importantly,  $f(k)$  does not depend on the mass of the halos. Photon perturbations on horizon scales also introduce scale dependence to the bias; the physics is identical to that of massive neutrinos (the presence of a free-streaming length) but the amplitude is much smaller because of the smaller photon energy density so it can be neglected. In fitting the parameters in eqs. (3)–(4) we use  $1.57 \times 10^{-3} \leq k/(h \text{ Mpc}^{-1}) \leq 5 \times 10^{-2}$ , and we have checked that our fits are insensitive to the precise value of  $k_{\text{max}}$ .

The red solid and green dashed lines show the best-fit models of scale-independent and scale-dependent linear bias to the simulations with massive neutrinos, respectively. The blue dot-dashed line displays the best-fit model of the scale-independent linear bias for the simulations without neutrinos. In the legend we show the reduced  $\chi_\nu^2$  values from the fit, which are computed using the *variance only*, as we do not have enough simulations to precisely measure the covariance matrix. We expect the covariance matrix to be highly diagonal on scales larger than  $0.05 h \text{ Mpc}^{-1}$ , but the reduced  $\chi_\nu^2$  values may be slightly underestimated. Thus, these numbers can serve as a guide to the goodness-of-fit, but they should not be used to compute  $p$ -values. We first examine the result for the massive neutrino simulations. It is clear, both visually and quantitatively through  $\chi_\nu^2$ , that for all halo catalogs, the scale-dependent linear bias model is a better fit to the data than the scale-independent linear

model for simulations with massive neutrinos. We emphasize that even if the halo bias is defined with respect to the CDM+baryon power spectrum, instead of total matter power spectrum as suggested by Refs. [21, 22], the scale dependence persists and extends to scales where nonlinearities are truly negligible. *This is the first time that scale-dependent linear halo bias is detected in simulations with massive neutrino perturbations*, hence further confirming the finding from separate universe simulations [9]. While we do not have measurements on scales larger than  $\sim 10^{-3} h \text{ Mpc}^{-1}$ , we nevertheless show the prediction for the scale-dependent bias there to illustrate that it ultimately approaches a constant with  $k$ , on scales where neutrinos have always clustered in the same way as CDM and baryons.

We next examine the results for the simulations without neutrinos. In all cases, the halo bias is statistically consistent with being scale independent. More importantly, as we move to larger scales, the data points become flatter, suggesting that there are no spurious scale-dependent features on the largest scale in our simulations.

The presence of the scale-dependent linear halo bias calls for more accurate modeling to extract neutrino information from the clustering statistics of biased tracers. The separate universe calculation, which provides a good model for the halo bias measured from our simulations, predicts that  $b_1^{\text{dep}}(k_\downarrow)/b_1^{\text{dep}}(k_\uparrow) \approx 1 + 0.25f_\nu$  and  $1 + 0.43f_\nu$  for halo populations with  $b_1^{\text{dep}}(k_\uparrow) = 1.7$  and  $3.5$ , respectively. Here,  $k_\downarrow$  and  $k_\uparrow$  denote wavenumbers in the asymptotic regimes on either side of the neutrino free-streaming scale. **Since the linear halo power spectrum is proportional to  $(b_1^{\text{dep}})^2$ , the neutrino effect will be doubled at the leading order compared to the raw bias.** The effect is therefore small, but *not* negligible in terms of  $f_\nu$  and there are important consequences. First, since the scale dependence of the linear bias is opposite to that of the CDM+baryon power spectrum (an increase, as opposed to suppression at higher  $k$ ), ignoring it can lead to an underestimation of  $f_\nu$ . Second, since the size of the effect depends on both  $f_\nu$  and  $b_1$ , it introduces a degeneracy between those parameters, which can degrade the constraints on  $f_\nu$ . On the other hand, this scale-dependent linear bias is a distinct signature of free-streaming particles that can exist only if there is an additional scale in the system. In the standard cosmological model, only massive neutrinos provide this large-scale characteristic length and so this signature offers a smoking gun for their detection.

Neutrinos also imprint a characteristic signature on the power spectrum: the change in the amplitude across the free-streaming scale. Yet detecting this signature is challenging because cosmic variance fundamentally limits the precision of measurements of the power spectrum on large scales. In contrast, measurements of a deterministic linear bias as seen in figure 1 are not limited by cosmic variance, but by the stochasticity between halos and the

<sup>5</sup> Alternatively,  $f(k)$  can be modeled from the spherical collapse in a region with a long-wavelength  $\delta_c(k)$  [8, 36], but for massive neutrinos the two approaches give equivalent predictions [9].



CDM+baryon field, which is thought to be small for halos of very high number density [52]. A detection of scale-dependent bias is therefore possible with even a small number of Fourier modes spanning the transition scales in figure 1 [45]. Moreover, the dependence of this effect on  $b_1$  allows for constraints on  $\sum m_\nu$  to be extracted from the ratio of the bias factors of two different galaxy populations within a single survey. Surveys that aim to constrain the bias at horizon-scales to study primordial physics may be of relevance [53].

Finally, we note that the separate universe formalism used to predict  $f(k)$  in eq. (4) and figure 1 also predicts a scale-dependent feature in the squeezed-limit bispectrum [9, 54]. Unfortunately that signal is much smaller and we estimate that roughly  $10\times$  more simulations are needed to confirm a detection.

## ACKNOWLEDGMENTS

Results in this paper were obtained using the Gordon cluster in the San Diego Supercomputer Center, the Rusty cluster at the Center for Computational Astrophysics, and the high-performance computing system at the Institute for Advanced Computational Science at Stony Brook University. CC was supported by grant NSF PHY-1620628. ML is supported by DOE DE-SC0017848. The work of FVN is supported by the Simons Foundation.

- 
- [1] D. J. Eisenstein and W. Hu, *Astrophys. J.* **511**, 5 (1997), [arXiv:astro-ph/9710252 \[astro-ph\]](#).
  - [2] W. Hu and D. J. Eisenstein, *Astrophys. J.* **498**, 497 (1998), [arXiv:astro-ph/9710216 \[astro-ph\]](#).
  - [3] N. Aghanim *et al.* (Planck), (2018), [arXiv:1807.06209 \[astro-ph.CO\]](#).
  - [4] N. Kaiser, *Astrophys. J.* **284**, L9 (1984).
  - [5] J. M. Bardeen, J. R. Bond, N. Kaiser, and A. S. Szalay, *Astrophys. J.* **304**, 15 (1986).
  - [6] P. Coles, *Mon. Not. Roy. Astron. Soc.* **262**, 1065 (1993).
  - [7] B. Mann, J. Peacock, and A. Heavens, *Mon. Not. Roy. Astron. Soc.* **293**, 209 (1998), [arXiv:astro-ph/9708031 \[astro-ph\]](#).
  - [8] M. LoVerde, *Phys. Rev.* **D90**, 083530 (2014), [arXiv:1405.4855 \[astro-ph.CO\]](#).
  - [9] C.-T. Chiang, W. Hu, Y. Li, and M. Loverde, *Phys. Rev.* **D97**, 123526 (2018), [arXiv:1710.01310 \[astro-ph.CO\]](#).
  - [10] A. Banerjee and N. Dalal, *JCAP* **1611**, 015 (2016), [arXiv:1606.06167 \[astro-ph.CO\]](#).
  - [11] J. Brandbyge and S. Hannestad, *JCAP* **1001**, 021 (2010), [arXiv:0908.1969 \[astro-ph.CO\]](#).
  - [12] S. Agarwal and H. A. Feldman, *Mon. Not. Roy. Astron. Soc.* **410**, 1647 (2011), [arXiv:1006.0689 \[astro-ph.CO\]](#).
  - [13] S. Bird, M. Viel, and M. G. Haehnelt, *Mon. Not. Roy. Astron. Soc.* **420**, 2551 (2012), [arXiv:1109.4416 \[astro-ph.CO\]](#).
  - [14] S. Hannestad, T. Haugbolle, and C. Schultz, *JCAP* **1202**, 045 (2012), [arXiv:1110.1257 \[astro-ph.CO\]](#).
  - [15] C. Wagner, L. Verde, and R. Jimenez, *Astrophys. J.* **752**, L31 (2012), [arXiv:1203.5342 \[astro-ph.CO\]](#).
  - [16] Y. Ali-Haïmoud and S. Bird, *Mon. Not. Roy. Astron. Soc.* **428**, 3375 (2012), [arXiv:1209.0461 \[astro-ph.CO\]](#).
  - [17] D. Inman, J. D. Emberson, U.-L. Pen, A. Farchi, H.-R. Yu, and J. Harnois-Déraps, *Phys. Rev.* **D92**, 023502 (2015), [arXiv:1503.07480 \[astro-ph.CO\]](#).
  - [18] J. Liu, S. Bird, J. M. Z. Matilla, J. C. Hill, Z. Haiman, M. S. Madhavacheril, A. Petri, and D. N. Spergel, *JCAP* **1803**, 049 (2018), [arXiv:1711.10524 \[astro-ph.CO\]](#).
  - [19] S. Bird, Y. Ali-Haïmoud, Y. Feng, and J. Liu, *Mon. Not. Roy. Astron. Soc.* **481**, 1486 (2018), [arXiv:1803.09854 \[astro-ph.CO\]](#).
  - [20] F. Villaescusa-Navarro, S. Bird, C. Pena-Garay, and M. Viel, *JCAP* **1303**, 019 (2013), [arXiv:1212.4855 \[astro-ph.CO\]](#).
  - [21] F. Villaescusa-Navarro, F. Marulli, M. Viel, E. Branchini, E. Castorina, E. Sefusatti, and S. Saito, *JCAP* **1403**, 011 (2014), [arXiv:1311.0866 \[astro-ph.CO\]](#).
  - [22] E. Castorina, E. Sefusatti, R. K. Sheth, F. Villaescusa-Navarro, and M. Viel, *JCAP* **1402**, 049 (2014), [arXiv:1311.1212 \[astro-ph.CO\]](#).
  - [23] M. Costanzi, F. Villaescusa-Navarro, M. Viel, J.-Q. Xia, S. Borgani, E. Castorina, and E. Sefusatti, *JCAP* **1312**, 012 (2013), [arXiv:1311.1514 \[astro-ph.CO\]](#).
  - [24] E. Castorina, C. Carbone, J. Bel, E. Sefusatti, and K. Dolag, *JCAP* **1507**, 043 (2015), [arXiv:1505.07148 \[astro-ph.CO\]](#).
  - [25] K. Heitmann *et al.*, *Astrophys. J.* **820**, 108 (2016), [arXiv:1508.02654 \[astro-ph.CO\]](#).
  - [26] H.-R. Yu *et al.*, (2016), [arXiv:1609.08968 \[astro-ph.CO\]](#).
  - [27] J. D. Emberson *et al.*, *Res. Astron. Astrophys.* **17**, 085 (2017), [arXiv:1611.01545 \[astro-ph.CO\]](#).
  - [28] J. Adamek, R. Durrer, and M. Kunz, *JCAP* **1711**, 004 (2017), [arXiv:1707.06938 \[astro-ph.CO\]](#).
  - [29] F. Villaescusa-Navarro, A. Banerjee, N. Dalal, E. Castorina, R. Scoccimarro, R. Angulo, and D. N. Spergel, *Astrophys. J.* **861**, 53 (2018), [arXiv:1708.01154 \[astro-ph.CO\]](#).
  - [30] M. Crocce, S. Pueblas, and R. Scoccimarro, *Mon. Not. Roy. Astron. Soc.* **373**, 369 (2006), [arXiv:astro-ph/0606505 \[astro-ph\]](#).
  - [31] M. Zennaro, J. Bel, F. Villaescusa-Navarro, C. Carbone, E. Sefusatti, and L. Guzzo, *Mon. Not. Roy. Astron. Soc.* **466**, 3244 (2017), [arXiv:1605.05283 \[astro-ph.CO\]](#).
  - [32] J. Brandbyge and S. Hannestad, *JCAP* **0905**, 002 (2009), [arXiv:0812.3149 \[astro-ph\]](#).
  - [33] V. Springel, *Mon. Not. Roy. Astron. Soc.* **364**, 1105 (2005), [arXiv:astro-ph/0505010 \[astro-ph\]](#).
  - [34] D. Blas, J. Lesgourgues, and T. Tram, *JCAP* **1107**, 034 (2011), [arXiv:1104.2933 \[astro-ph.CO\]](#).
  - [35] J. Lesgourgues and T. Tram, *JCAP* **1109**, 032 (2011), [arXiv:1104.2935 \[astro-ph.CO\]](#).
  - [36] J. B. Muñoz and C. Dvorkin, *Phys. Rev.* **D98**, 043503 (2018), [arXiv:1805.11623 \[astro-ph.CO\]](#).
  - [37] Ya. B. Zeldovich, *Astron. Astrophys.* **5**, 84 (1970).
  - [38] F. Villaescusa-Navarro, J. Miralda-Escudé, C. Peña-Garay, and V. Quilis, *JCAP* **1106**, 027 (2011), [arXiv:1104.4770 \[astro-ph.CO\]](#).
  - [39] K. Ichiki and M. Takada, *Phys. Rev.* **D85**, 063521 (2012), [arXiv:1108.4688 \[astro-ph.CO\]](#).
  - [40] M. LoVerde, *Phys. Rev.* **D90**, 083518 (2014),

- arXiv:1405.4858 [astro-ph.CO].
- [41] L. Senatore and M. Zaldarriaga, (2017), arXiv:1707.04698 [astro-ph.CO].
  - [42] S. P. D. Gill, A. Knebe, and B. K. Gibson, *Mon. Not. Roy. Astron. Soc.* **351**, 399 (2004), arXiv:astro-ph/0404258 [astro-ph].
  - [43] S. R. Knollmann and A. Knebe, *Astrophys. J. Suppl.* **182**, 608 (2009), arXiv:0904.3662 [astro-ph.CO].
  - [44] S. Vagnozzi, T. Brinckmann, M. Archidiacono, K. Freese, M. Gerbino, J. Lesgourgues, and T. Sprenger, *JCAP* **1809**, 001 (2018), arXiv:1807.04672 [astro-ph.CO].
  - [45] M. LoVerde, *Phys. Rev.* **D93**, 103526 (2016), arXiv:1602.08108 [astro-ph.CO].
  - [46] A. Raccanelli, L. Verde, and F. Villaescusa-Navarro, *Mon. Not. Roy. Astron. Soc.* (2018), 10.1093/mnras/sty2162, arXiv:1704.07837 [astro-ph.CO].
  - [47] M. Schmittfull and U. Seljak, *Phys. Rev.* **D97**, 123540 (2018), arXiv:1710.09465 [astro-ph.CO].
  - [48] R. K. Sheth and G. Tormen, *Mon. Not. Roy. Astron. Soc.* **308**, 119 (1999), arXiv:astro-ph/9901122 [astro-ph].
  - [49] V. Assassi, D. Baumann, D. Green, and M. Zaldarriaga, *JCAP* **1408**, 056 (2014), arXiv:1402.5916 [astro-ph.CO].
  - [50] M. Biagetti, V. Desjacques, A. Kehagias, and A. Riotto, *Phys. Rev.* **D90**, 045022 (2014), arXiv:1405.1435 [astro-ph.CO].
  - [51] E. Giusarma, S. Vagnozzi, S. Ho, S. Ferraro, K. Freese, R. Kamen-Rubio, and K.-B. Luk, (2018), arXiv:1802.08694 [astro-ph.CO].
  - [52] U. Seljak, *Phys. Rev. Lett.* **102**, 021302 (2009), arXiv:0807.1770 [astro-ph].
  - [53] O. Doré *et al.*, (2014), arXiv:1412.4872 [astro-ph.CO].
  - [54] C.-T. Chiang, Y. Li, W. Hu, and M. LoVerde, *Phys. Rev.* **D94**, 123502 (2016), arXiv:1609.01701 [astro-ph.CO].